Accepted Manuscript

Bacterial diversity in typical abandoned multi-contaminated nonferrous metal(loid) tailings during natural attenuation

Jian-li Liu, Jun Yao, Fei Wang, Ning Min, Ji-hai Gu, Zi-fu Li, Geoffrey Sunahara, Robert Duran, Tatjana Solevic Knudsen, Karen A. Hudson-Edwards, Lena Alakangas

Please cite this article as: Liu, J.-l., Yao, J., Wang, F., Min, N., Gu, J.-h., Li, Z.-f., Sunahara, G., Duran, R., Knudsen, T.S., Hudson-Edwards, K.A., Alakangas, L., Bacterial diversity in typical abandoned multi-contaminated nonferrous metal(loid) tailings during natural attenuation, *Environmental Pollution* (2019), doi: https://doi.org/10.1016/j.envpol.2018.12.045.

Graphic abstract

Bacterial diversity in typical abandoned multi-contaminated nonferrous metal(loid) tailings during natural attenuation

Jian-li Liu [a], Jun Yao [b] [*], Fei Wang [a], Ning Min [b], Ji-hai Gu [b], Zi-fu Li [a] [**],

Geoffrey Sunahara [b,c], Robert Duran [b,d], Tatjana Solevic Knudsen [e],

Karen A. Hudson-Edwards [g] and Lena Alakangas [h]

[a] School of Energy and Environment Engineering, University of Science and Technology Beijing, Beijing 100083, China

[b] School of Water Resource and Environment Engineering, China University of Geosciences (Beijing) 100083, China

[c] Department of Natural Resource Sciences, McGill University, Montreal, Quebec, H9X3V9, Canada

[d] Equipe Environnement et Microbiologie, MELODY group, Université de Pau et des Pays de l'Adour, E2S-UPPA, IPREM UMR CNRS 5254, BP 1155, 64013 Pau Cedex, France

[e] Institute of Chemistry, Technology and Metallurgy, University of Belgrade, Njegoseva 12, PO Box 473, 11001 Belgrade, Serbia

[f] Department of Applied Chemistry, Szent István University, Villányi út 35-43, 1118 Budapest, Hungary

[g] Environment & Sustainability Institute and Camborne School of Mines, University of Exeter, Penryn, Cornwall TR10 9DF, UK

[h] Lule University of Technology, -971 87 Lule1, Sweden

* Corresponding Author. School of Water Resource and Environment Engineering, China University of Geosciences (Beijing), 29 Xueyuan Road, Haidian District, 100083 Beijing, China, E-mail: yaojun@cugb.edu.cn (J. Yao), Tel: +86-10-82321958

** Corresponding Author. School of Energy and Environment Engineering, University of Science and Technology Beijing, 30 Xueyuan Road, Haidian District,100083 Beijing, China, E-mail: zifulee@aliyun.com (Z.F. Li), Tel: +86-10-62334378

Abstract

Abandoned nonferrous metal(loid) tailings sites are anthropogenic, and represent unique and extreme ecological niches for microbial communities. Tailings contain elevated and toxic content of metal(loid)s that had negative effects on local human health and regional ecosystems. Microbial communities in these typical tailings undergoing natural attenuation are often very poorly examined. The diversity and inferred functions of bacterial communities were examined at seven nonferrous metal(loid) tailings sites in Guangxi (China), which were abandoned between 3 and 31 years ago. The acidity of the tailings sites rose over 31 years of site inactivity. *Desulfurivibrio*, which were always coupled with sulfur/sulfide oxidation to dissimilate the reduction of nitrate/nitrite, were specific in tailings with 3 years abandonment. However, genus beneficial to plant growth (*Rhizobium*), and iron/sulfur-oxidizing bacteria and metal(loid)-related genera (*Acidiferrobacter* and *Acidithiobacillus*) were specific within tailings abandoned for 23 years or more. The increased abundance of acid-generating iron/sulfur-oxidizing and metal(loid)-related bacteria and specific bacterial communities during the natural attenuation could provide new insights for understanding microbial ecosystem functioning in mine tailings. OTUs related to *Sulfuriferula*, *Bacillus*, *Sulfurifustis*, *Gaiella*, and *Thiobacillus* genera were the main contributors differentiating the bacterial communities between the different tailing sites. Multiple correlation analyses between bacterial communities and geochemical parameters indicated that pH, TOC, TN, As, Pb, and Cu were the main drivers influencing the bacterial community structures. PICRUSt functional exploration revealed that the main functions were related to DNA repair and recombination, important functions for bacterial adaptation to cope with the multi-contamination of tailings. Such information provides new insights to guide future metagenomic studies for the identification of key functions beyond metal-transformation/resistance. As well, our results offers novel outlooks for the

61   management of bacterial communities during natural attenuation of multi-contaminated

62   nonferrous metal(loid) tailings sites.

63

64   **Keywords:** bacterial community succession; metal(loid)s; natural attenuation;

65   nonferrous metal(loid) tailings

66   **1. Introduction**

67   Mine tailings repositories are unwanted and uneconomic materials from the

68   mineral processing deposited exposure in the air. Tailings often contain elevated

69   concentrations of metal(loid)s, which are potentially toxic (Lecumberri-Sanchez et al.,

70   2014; Hudson-Edwards, 2016). Abandoned nonferrous metal(loid) tailings (i.e.,

71   facilities having no operator or successor) have received considerable attention around

72   the world because they represent a risk for the environment and human health

73   (Aleksandrovskii et al., 2015; COM, 2016). Guangxi (China) is one of the

74   predominant nonferrous mining areas in the world (Rademaekers et al., 2011). It is a

75   karst landform with many ecologically sensitive areas and is located upstream of the

76   Pearl River Basin (China's third longest river and second largest by volume) (Wang et

77   al., 2007). In Guangxi, different mining activities release waste that results in the

78   formation of tailings with heterogeneous composition containing high concentrations

79   of metal(loid)s and flotation reagents (Liu et al., 2018). Such level of

80   multi-component contamination is probably more serious than many other areas in the

81   world (Zhu et al., 2018).

82   Biotic and abiotic processes modify the speciation of metal(loid)s and

83   physical-chemical characteristics in tailings (Ye et al., 2017a; Ye et al., 2017b), which

84   facilitate metal(loid)s permeation into soil, surface runoff, and air transportation

85   (Deng et al., 2009; COM, 2016; Jiang et al., 2016; Yi et al., 2016; Yuan and Liu,

86   2016). Natural attenuation occurs when natural processes (including pedogenesis) are

87   managed to recover an ecosystem to a point where the original fauna and flora are

88   replicated (Clewell, 2000). Natural attenuation is more economical for re-purposing

89   tailings compared to physical remediation, reclamation processes, or activated biochar

90   addition on remediation (Lima et al., 2016, Ye et al., 2019). However, natural

91 attenuation is a slow process that can take more than 100 years (Bradshaw, 1997;

92 Ciarkowska et al., 2016; Lima et al., 2016). With time, microbial colonization follows

93 the modification of physical-chemical parameters (Giloteaux et al., 2013) due to

94 bio-geochemical processes (Haferburg and Kothe, 2007). Knowledge of the

95 colonization of microbial communities during natural attenuation in mine tailings is

96 limited (Bruneel et al., 2008; Volant et al., 2014; Zhan and Sun, 2014; Chao et al.,

97 2016), particularly in the Guangxi area where only three tailings sites (Pb-Zn and Mn

98 sites) have been investigated (Jin et al., 2015; Liu et al., 2014; Li et al., 2015). Recent

99 results show that the distribution of bacterial communities in Guangxi nonferrous

100 metal(loid)s tailings was best correlated with the combination of pH, Cu, Pb, and Mn,

101 suggesting that these parameters influence the organization of bacterial communities

102 (Liu et al., 2018). However, the modification of bacterial communities during natural

103 attenuation in undisturbed nonferrous metal(loid) tailings is still uninvestigated.

104   To address this research gap, we examined nonferrous mine tailings sites with

105 different periods of abandonment (from 3 to 31 years) in the Guangxi mining area

106 (Fig. 1 and Table S1), which have different geochemical characteristics. We

107 hypothesize that temporal changes in biogeochemical factors, and bacterial diversity

108 and metabolic functions are part of the natural attenuation process occurring in these

109 tailings. The present study offers the possibility to examine the ecological changes,

110 such as primary succession of microbial communities during natural attenuation. The

111 objectives of this study were to: (1) investigate the structure of the microbial

112 community (by MiSeq sequencing of 16S rRNA genes) and predict the metabolic

113 functions in mine tailings, and (2) analyze the combined effects of geochemical

114 factors including pH, total organic carbon (TOC), total nitrogen (TN), total

115 phosphorus (TP), and metal(loid)s content on the bacterial community structure. This

116 study will provide a better understanding of microbial variations in nonferrous mine

117 tailings, and useful information for the management of bacterial resources during

118 natural attenuation of nonferrous metal(loid) tailings.

119

120 **2. Materials and methods**

121 **2.1 Site description and sampling**

122   Sampling was performed around Hechi City of Guangxi (China) (Fig. 1), which

123 has a subtropical monsoon climate (Bi et al., 2016). Seven tailings sites with different

124 composition and ages (ranging from three to 31 years old) were sampled to evaluate

125 changes in bacterial communities during the natural attenuation (Fig. 1). The

126 abandonment periods were determined using tailings pond records from the local

127 Environmental Protection Agency. The types of tail sand at these seven tailings sites

128 were mainly from Sb, Pb-Zn, and Sn mining and smelting industries (Table S1).

129 These tailings were not treated with amendments or any remediation technology.

130 There was no visible plant growth in all of the studied sites.

131   Surface samples (0-10 cm) with 3-10 subsamples for each site were collected in

132 June 2016, using a wooden shovel according to EU international guideline (Hansen et

133 al., 2007). All samples were directly placed into plastic pipes in cooler boxes (at 4°C)

134 and transported to laboratory at the University of Science and Technology Beijing

135 within 2 d of sampling. After thorough homogenization, the samples were split into

136 two parts. Approximately 500 g for each sample was then stored at -20°C until DNA

137 extraction. The remaining samples were used for geochemical analyses, and were

138 stored at 4°C.

139   < insert Fig. 1 >

140

141 **2.2 Analysis of geochemical factors**

142   Samples were air-dried and analyzed according to the technical specifications for

143 soil analysis for determination of pH, total organic carbon (TOC), total nitrogen (TN),

144 and total phosphorus (TP) as defined by the China National Agricultural Technology

145 Extension Center (2006). The operating conditions for the TOC solid sample module

146 (SSM-5000A, Shimadzu) were: the oven temperature, 680°C, and the gas flow of

147 high purity oxygen in TOC-V and SSM-5000A section, 150 and 500 mL/min,

148 respectively. Samples were extracted with a solution of nitric, hydrochloric, and

149 hydrofluoric acids (5:3:2, v/v/v) in a microwave unit to determine the total

150 metal(loid)s content (T-M). The acid soluble fraction of metal(loid)s (H-M) were

151 analyzed using the Chinese method HJ/T299-2007. This fraction of H-M represents

152 the leachable compartment that could be released into the environment. The leaching

153 solution was prepared by adding 0.09 mL of a solution of sulfuric and nitric acids (2:1,

154 v/v) and taken up to 1 L with ultra-pure water (Milli-Q Academic Lab Water System,

155 Millipore, USA). Certified reference materials of soil samples (GBW 07405 (GSS-5))

156 and polymetallic ore samples (GBW 07162 (GSO-1)) were used for quality control.

157 The limit of detection (LOD) for T-Ms was $> 0.10 \times 10^{-3}$ mg/kg (Liu et al., 2018) and

158 for H-Ms was > 0.10 mg/kg (Wang, 2018), according to the China Environmental

159 Monitoring Technical guideline (HJ 168-2010). The recoveries were between 85% -

160 110%. Samples were placed into 20 mL of leaching solution (pH 3.20 ± 0.05) and

161 shaken for about 20 h. Induced coupled plasma optical emission spectrometry

162 (ICP-OES) (iCAP 7000 SERIES, Thermo Scientific) was used to determine the

163 metal(loid)s concentrations. The operating conditions were: auxiliary gas flow, 0.5

164 L/min; plasma gas stable time, 10 min; ICP RF power, 1150 W; and pump rate, 45

165 rpm. All the samples were sieved at 100-mesh size (0.149 mm, US standard) to

166   determine the geochemical factors. The analyses were performed in duplicate to

167   evaluate precision.

168

169   **2.3 MiSeq sequencing and data processing**

170   Genomic DNA was extracted using the SoilGen DNA Kit (CWBio, Bejing,

171   China). DNA extraction kits allow to obtain high-quality DNA for PCR amplification

172   and sequencing (Bordenave et al., 2004; Bordenave et al., 2008). The potential

173   damage during DNA extraction are prevented by diluting metal(loid)s and eliminating

174   them in the first steps of the procedure allowing molecular analyses of highly

175   contaminated samples such as acid mine drainage (Giloteaux et al., 2010). The

176   universal primer set 338F/806R amplified the V3-V4 region of the bacterial 16S

177   rRNA gene, and an 8 bp-tag was used for the sample identification (Liu et al., 2016).

178   Polymerase chain reaction (PCR) amplification (20 μL) was conducted in triplicate

179   and contained 10 ng DNA template, 4 μL of $5 \times$ FastPfu Buffer, 2 μL of 2.5 mM

180   dNTPs, 0.2 μM of each primer, 0.4 μL FastPfu Polymerase, 0.2 μL bovine serum

181   albumin, and double-distilled water. PCR was started with an initial denaturation (3

182   min at 95°C), followed by 28 cycles of denaturation (30 s at 95°C), annealing (30 s at

183   55°C), and extension (45 s at 72°C), and a final extension (10 min at 72°C).

184   Sequencing using a MiSeq platform was performed at a commercial facility

185   (Shanghai Majorbio Bio-Pharm Technology Corporation, Shanghai, China).

186   All the 16S raw data were trimmed and filtered using Trimmomatic software

187   (Manual v0.32), by trimming the average base quality region below 20 bp (Trujillo et

188   al., 2014). The paired-end reads were merged using FLASH software. The sequences

189   assigned to chloroplasts, mitochondria or eukaryotes were removed in the

190   pretreatment of raw reads. Bacterial operational taxonomic units (OTUs) were

191   clustered with 97% similarity using Usearch version 7.0 (http://drive5.com/uparse/)

192   based on Silva Release128 (http://www.arb-silva.de). Taxonomy was assigned to

193   OTUs using Qiime (http://qiime.org/scripts/assign_taxonomy.html) and ribosomal

194   database project pipeline classification algorithm with a 70% confidence threshold

195   (Nakayama, 2010). Alpha diversity indices (ace, Shannon, Simpson evenness and

196   Boneh) and hierarchical clustering were calculated with Qiime. Circos-0.67-7 was

197   used to perform the bacterial composition of each sample, and the distribution ratio of

198   dominant bacteria in different samples. Functional prediction of bacterial

199   communities was determined using PICRUSt, a well-documented tool to assign

200   sequencing information based on 16S input data to reveal the functions encoded in

201   bacterial communities (Langille et al., 2013; Mchardy et al., 2013). Kyoto

202   Encyclopedia of Genes and Genomes (KEGG) databases (e-value cut-off 10^{-5}) were

203   used for functional annotation and metabolism analyses (Mchardy et al., 2013;

204   Kanehisa et al., 2014; Vrutika et al., 2016). The weighted nearest sequenced taxon

205   index (NSTI) was calculated to assess the accuracy of PICRUSt analysis (Langille et

206   al., 2013).

207

208   **2.4 Statistical analyses**

209   One-way ANOVA was applied to test the differences of geochemical factors; a

210   level of $p < 0.05$ was considered significant. The relationships between geochemical

211   factors and alpha-diversity indexes were analyzed using Spearman correlation (SPSS

212   v21). SIMPER analysis based on Bray-Curtis similarity measurement was used to test

213   microbial differences in the tailings. Non-metric multidimensional scaling (NMDS)

214   and distance-based redundancy analysis (db-RDA) analysis were conducted to test the

215   correlation between bacterial communities and geochemical factors of tailings sites

216   based on weighted normalized unifrac distance algorithm. The significance of

217   geochemical factor was tested with Monte Carlo permutations (permu = 999).

218   Correlations of each bacterial community and each geochemical factor were

219   calculated with p-values < 0.05 and plotted as a heatmap. Network analysis was used

220   to reflect the relationship between tailings sites and genera. After detection for genera

221   (Gephi software), each module was represented by network correlation shared values

222   of abundance profile by using modularity analysis. BIOENV analysis was used to

223   determine the combined effects of geochemical factors on the metabolic pathways of

224   bacterial communities. All the analyses were done using R software (v 3.4.1) unless

225   otherwise stated.

226

227   **3. Results and discussion**

228   **3.1 Geochemical parameters of nonferrous mine tailings samples**

229   The pH in the seven studied tailings (Table S1) decreased with the period of

230   abandonment, notably around pH 7.3 at the youngest sites (from T_3Y to T_15Y),

231   weakly acidic (pH 6.4) at site T_23Y, and extremely acidic (pH 2.6) at site T_31Y.

232   This is consistent with other reports showing that the pH decreased in mine tailings

233   undergoing more than 30 years of natural attenuation (Huang et al, 2011; Zhan and

234   Sun, 2014; Ciarkowska et al., 2016). The gradual acidification of tailings could be

235   caused by microbial mediated oxidative dissolution of pyrite (FeS_2) and other sulfide

236   minerals exposed to air and water during natural attenuation (Huang et al., 2016). The

237   low nutrient concentrations of C/N/P could nevertheless support the observed growth

238   of microorganisms (described below), at least during the early phases of natural

239   attenuation (Oudjehani, et al., 2002).

240   As expected at nonferrous metal(loid) tailings sites, the total metal(loid)s

241 contents (T-M) were higher compared with the reported tailing sites in other regions

242 around the world (Alakangas et al. 2010; Giloteaux et al., 2013; Bruneel et al., 2017).

243 The total arsenic content (T-As) was significantly correlated with total contents of Cd,

244 Cr, and Zn (Spearman rho = from -0.82 to 0.86, $p < 0.04$; Table 1). Similar

245 correlations between As, Zn, and Cd have been reported at mining- and

246 alumina-contaminated soils (Zacháry et al., 2015).

247   The acid soluble fraction of metal(loid)s (H-M), representing the leachable

248 fraction, was generally higher in tailing sites with 31 years abandonment (Table S1).

249 Significant differences were also observed among the tailings sites, particularly for

250 H-Cd, H-Cr, and H-Cu (ANOVA, $p < 0.05$, Table S1). Acid-soluble fraction in

251 surface tailings represents the elements releasable that can migrate laterally or

252 downwards via biotic and abiotic processes (Alakangas et al. 2010; Volant et al.,

253 2014). The increased concentration of H-Ms and decreased pH with the age of

254 abandonment suggested that a release of these metal(loid) was increasing over time,

255 which was reported for other tailings (Walder and Chavez, 1995; Shu et al., 2001).

256   < Insert Table 1 >

257

258 **3.2 Microbial community diversity and composition of nonferrous mine tailings**

259   To determine the bacterial dynamics in abandoned tailings, a total of 1,481

260 bacterial OTUs were identified of all quality 16S rRNA bacterial sequences (265,487

261 in total) after removing singletons and chimeric sequences (Tables S2 and S3). These

262 1,481 OTUs represent a high coverage (99.8 ± 0.1 %, Table S2), indicating that the

263 sequencing data could reflect the vast majority of microbial diversity in the real

264 environment. Furthermore, the Shannon diversity indexes were between 2.88 - 4.80,

265 which were similar to an earlier report of a Pb-Zn mining site (Chen et al., 2013).

266   Bacterial diversity showed a decreasing relationship with the age of abandonment

267   (Table S2 and Fig. S1). Nevertheless, the bacterial richness (Table S2) was up to eight

268   times higher than that reported in an abandoned Pb-Zn mine tailing site (Epelde et al.,

269   2015), but no significant trend could be observed with abandonment age. This could

270   be due to some more fundamental properties of tailings such as tailing matrix, mineral

271   phases, and chemical composition since the tailings are from different types of mining

272   and smelting industries (Fig. S1). In contrast, Chao et al. (2016) reported clear

273   differences, as well as a time-dependent increase, in bacterial richness among REE

274   (Rare Earth Elements) tailings sites that were abandoned for 3, 6, and 10 years. The

275   richness of bacterial communities had a significant correlation with PD (phylogenetic

276   diversity, $rho = 0.972$, $p = 0.0002$; Table 1), which was statistically correlated with

277   TP ($rho = 0.79$, $p = 0.036$; Table 1). Overall, our results indicated a high genetic

278   diversity in the Guangxi nonferrous mine tailings sites.

279   Over 98% of the OTUs could be assigned to a taxonomic phylum with 70%

280   confidence; while over 56% of sequences were generally identified as no-rank or

281   unclassified genera (Table S3), which was lower than that in a Sb-rich tailings dump

282   (Xiao et al., 2016). Coupled with the high coverage and sequencing depth (99.8 ±

283   0.1 %, Table S2), this low assigned rate suggested these tailings sites had vast

284   unidentified populations and microbial resources. These results were consistent with

285   an earlier report showing that 58% of the sequences in a vanadium- and 17% in a

286   gold- mine water from a South African mine, could not be assigned to a particular

287   phylum (Keshri et al., 2015). Specifically, the shared phyla of tailings sites were

288   Proteobacteria, Firmicutes, and Actionobacteria, accounting for 76% of total

289   microbial community (Fig. 2), which confirmed recent studies by Liu et al. (2018) at

290   abandoned nonferrous metal tailings sites, and by Chao et al (2016) at an abandoned

291   REE tailings facility. These studies reported the same or similar dominant bacterial

292   communities (at the phylum level), despite differences in pH and geochemical factors

293   of the tailings.

294   < insert Fig. 2 >

295   Among the total 507 genera identified from the seven tailings sites, 31 shared

296   genera (relative abundance > 1% of total sequences at least in one tailing site) had

297   different abundance among the seven tailings sites (Table S4). The differences

298   observed were mainly due to different abundances of *Sulfuriferula*, *Bacillus*,

299   *Sulfurifustis*, *Gaiella*, and *Thiobacillus* (Table 2). *Sulfurifustis* and *Thiobacillus* were

300   the most abundant genera shared by tailings sites that were abandoned for < 15 years

301   (Table S4), indicating that these two genera may have contributed to sulfur- and iron

302   oxidation at these sites. To date only three studies have detected *Sulfurifustis* that

303   could be involved in sulfur oxidation (Kojima, et al., 2015; Kojima, et al., 2016;

304   Umezawa, et al., 2016). *Thiobacillus* is capable of iron/sulfur-oxidization and

305   carbon/nitrogen fixation in the early stages of the acidification processes of tailings

306   (Yamanaka, 1996; Huang et al., 2016). *Ralstonia*, the most abundant genus in tailing

307   sites abandoned for up to 23 years (29%; Table S4), is a ubiquitous inhabitant of soil,

308   freshwater and even ultrapure water in industrial systems (Gan, et al., 2012). This

309   genus carries metal resistant genes, such as *czc* (resistance to cadmium, zinc, and

310   cobalt) and *ncc* (cobalt and cadmium) (Mergeay, et al., 2010). *Acidithiobacillus* was

311   most abundant at the extremely acidic tailing site (pH = 2.0, Table S1) abandoned for

312   31 years (accounting for 29% of total communities, Table S4). This genus was found

313   to be able of carbon/nitrogen fixation, iron/sulfur oxidation, and arsenic oxidation

314   (Huang et al., 2016). *Acidithiobacillus* may play an important role in the iron and

315   arsenic oxidation in late acidification of the present tailing sites as reported for other

316 tailings sites (Bruneel et al., 2005; Jorge et al., 2008; Huang et al., 2016).

317 < insert Table 2 >

318

319 **3.3 Structure of tailings microbial communities**

320 Although the tailings sites shared bacterial populations, the whole bacterial

321 structures were different (Fig. 3). Correlation analysis of geochemical factors and

322 bacterial structure of tailings revealed four cluster groups: i) OTUs in T_4Y, T_8Y,

323 and T_15Y correlated with TOC, ii) OTUs in T_6Y correlated with TN, T-As, and

324 H-Pb, iii) OTUs in T_23Y correlated with pH and H-Sb, and iv) OTUs in T_31Y

325 correlated with pH and TP (Fig. 3). These findings were consistent with earlier studies

326 indicating that pH, total metal(loid)s, and acid leachable metal(loid)s were correlated

327 with microbial communities in tailings sites (Bruneel et al., 2017; Gupta et al., 2017;

328 Hao et al., 2017). The acid leachable or bio-accessible fractions of metal(loid)s (such

329 as H-Pb) can easily migrate with applications of acid rain or during natural

330 acidification, and this process can be accelerated by the metabolic processes of

331 adapted microbial communities (Haferburg and Kothe, 2007). For example, to survive

332 in aquatic and soil environments with Pb^{2+} contamination, some microbes have

333 developed Pb^{2+} resistance, involved extracellular binding, intracellular sequestration,

334 active transport, and exclusion by forming a permeable barrier (Pan et al., 2017).

335 < insert Fig. 3 >

336 Specific genera in each tailing site were also observed (Fig. 4A), suggesting that

337 these tailings sites represent unique ecological niches during tailing colonization and

338 natural attenuation. The distribution of these genera correlated with a combination of

339 pH, TOC, H-Pb, and T-As (rM = 0.80, p = 0.01; Fig. 4B; Table 3), indicating that

340 these four geochemical factors may play a key role in the distribution of microbial

341 communities. In tailing sites with 3 years abandonment, *Desulfurivibrio* were specific

342 (Fig. 4A), which always grow chemolithotrophically by sulfur/sulfide oxidation and

343 dissimilate the reduction of nitrate/nitrite in slight alkali environments (Sorokin et al.,

344 2008; Thorup et al., 2017). Although no plants were observed at the tailings sites,

345 specific *Rhizobium* genus, beneficial for plant growth (Sujkowska-Rybkowska and

346 Ważny, 2018), were observed in site T_23Y. This observation could be explained by

347 aerial seeding by plants from the surrounding areas. The distribution of bacterial

348 communities in T_23Y was correlated with pH and H-Sb content (Fig. 3B). In the

349 extremely acidic T_31Y tailing site, most of the specific genera, such as

350 *Acidithiobacillus* and *Acidiferrobacter*, were related to sulfur/iron oxidation (Fig. 4A).

351 These genera had significant and negative correlations with pH, and significant

352 positive correlations with H-As, H-Cr, and H-Cu contents ($p < 0.001$, Fig. 5). This

353 observation would be expected because *Acidiferrobacter* and *Acidithiobacillus*

354 species participate in the metabolism of iron, sulfur, arsenic, and organic matter (Fan

355 et al., 2016; Bruneel et al., 2017). In addition, acidophilic *Acidithiobacillus*-related

356 sequences can generate AMD waters, and oxidize the ferrous sulfate to immobilize

357 As^{5+} in arsenic-contaminated soil (Huang et al., 2016; Yang et al., 2017), suggesting

358 that this species may have an important ecological role for increasing metal sulfide

359 dissolution and controlling AMD production. The frequently encountered distribution

360 and numerous dominance of iron/sulfur-oxidizing and metal-related genera in acidic

361 environments during the long process of natural attenuation reflects their potential

362 role in the natural attenuation of metal(loid)s and generating AMD at tailings sites

363 (Chen et al., 2013; Huang et al., 2016).

364   < insert Fig. 4 >

365   < insert Fig. 5 >

366 < insert Table 3 >

367 Chao et al. (2016) showed that soil microbiota can vary significantly at different

368 abandoned REE tailing sites, by the co-development of microbial and plant

369 communities during natural attenuation. These studies showed that site-specific

370 factors induced microbial changes within subgroups of abandoned sites, which is

371 consistent with our findings. However, the tailing samples in the Chao et al. (2016)

372 contained vegetal material compared to the present study. Therefore, it is not known if

373 the microbial changes described in the Chao et al. study are related to site factors or

374 plant development, or both. Ridl et al. (2016) demonstrated that plants, and not the

375 use of fertilizers, were the drivers of microbial community structure in contaminated

376 soil, with the magnitude of effect depending on the type of plant species. Based on

377 our study, in which plants were not observed, it is likely that microbial changes were

378 caused by geochemical factors and the extremely unfavorable growing conditions

379 (such as low C/N/P contents and high metal(loid)s concentrations).

380

381 **3.4 Potential functional metabolism of bacterial communities**

382 For successful survival and adaptation to a multi-contaminated environment,

383 which constitutes an evolutionary challenge for organisms, sophisticated resistance

384 strategies and mechanisms are required for microbial succession (Guan et al., 2017).

385 PICRUSt analysis was used for exploring the possible metabolism pathways

386 associated with the detoxification of metal(loid)s and transport of geochemical

387 elements in tailings undergoing natural attenuation. The NSTI (nearest sequenced

388 taxon index) values in the present study were less than 0.18 (except at site T_3Y)

389 indicating that the PICRUSt prediction analysis was accurate (Table S2). The

390 relationship between the KEGG pathways and bacterial community structures

391   revealed that each tailing site had its specific functional pathways (Fig. 6). KEGG

392   pathways related to DNA replication and repair, and recombination proteins were

393   mainly clustered close to tailing sites with 31 years natural attenuation (Fig. 6). As

394   well, the distribution of these predicted functional metabolic pathways was strongly

395   correlated with pH, TOC, TP, T-As, T-Zn, and H-Cr ($r = 0.98$, Table S7). It is known

396   that environmental stresses (such as pH, As, and Pb) can directly or indirectly damage

397   the structure of DNA, which results in the mismatch of nucleic acids, and DNA

398   degradation, thus affecting the diversity and structure of microorganisms

399   (Amaral-Zettler et al., 2011; Bruneel et al., 2017; Guan et al., 2017; Hao et al., 2017).

400   These in turn could ultimately lead to microbial cell injury, protein degradation, and

401   gene mutation (Dai et al., 2013; Guan et al., 2017). It is possible that the DNA repair

402   system participated in the sensitive targets of microbial metal(loid)s toxicity observed

403   in our study, resulting in the adaptation of bacterial communities to the extreme

404   tailings environments.

405   SIMPER analysis using the KEGG database indicated that the metabolic

406   pathways directly related to ATP, methane, nitrogen, and energy generation (such as

407   ABC transporters) also contributed to the differences of bacterial community

408   structures in the seven tailings sites (Table S5 and S6). ABC transporters constitute

409   large amounts of membrane proteins and could transport many diverse substrates,

410   such as metal(loid)s and secondary metabolites (Theodoulou and Kerr, 2015). As

411   discussed above, metal(loid) oxidation-related genus of *Acidithiobacillus* could also

412   encode the ABC transporter genes involved with zinc ion transport (Hou et al., 2012).

413   Previous studies also confirmed that genetic expression of iron/sulfur-oxidizing and

414   metal(loid) tolerance may propagate through horizontal gene transfer (Sandoval et al.,

415   2004; Bouzat and Hoostal, 2013), which enables bacterial communities to acquire a

416   gene (or genes) favoring the adaptation of bacterial communities to extreme

417   environments during natural attenuation. To better understand the mechanisms of

418   bacterial communities undergoing natural attenuation in nonferrous metal tailings,

419   further analyses combining geochemical parameters (such as inorganic C,

420   sulfides/sulfates/iron contents, and the neutralization capacity) with

421   metatranscriptomic and metagenomic analyses will provide useful information.

422

423   **Conclusions**

424   Our study provides greater insight into the temporal dynamics of bacterial

425   communities during natural attenuation. Each tailing site was identified as a unique

426   ecological niche. Tailings abandoned for ≤ 15 years were in a pre-acidification phase

427   and undergoing acidification. Tailings ≥ 23 years abandonment had higher acid

428   soluble As concentrations and the metal(loid)s that may represent a risk for human

429   health and the environment (COM, 2016; Hudson-Edwards, 2016). A gradual

430   succession of bacterial genera in the tailings sites was observed suggesting that the

431   bacterial communities become more acidophilic and metal-resistant. Functional

432   metabolic pathways of DNA repair and recombination may be the main potential

433   mechanisms for the microbes to cope with oligotrophic and extreme tailings habitats.

434   The present study suggests that although natural attenuation may be a key strategy

435   towards sustainability, careful monitoring of abandoned tailings sites should be

436   considered as early as possible, to enable the timely management of any potential

437   environmental risks present at these sites.

438

451 **Appendix A. Supporting information**

452 Supplementary data related to this article can be found at the website of

453 *Environmental Pollution*.

454

455 **References**

456 Alakangas L., Lundberg A., Öhlander B., 2010. Estimation of temporal changes in
457   oxidation rates of sulphides in copper mine tailings at Laver, northern Sweden.
458   Sci Total Environ 408, 1386-1392.
459 Aleksandrovskii, A.L., Aleksandrovskaya, E.I., Dolgikh, A.V., 2015. Soils and
460   cultural layers of ancient cities in the south of European Russia. Eurasian Soil
461   Sci 48, 1171-1181.
462 Amaral-Zettler, L.A., Zettler, E.R., Theroux, S.M., et al., 2011. Microbial community
463   structure across the tree of life in the extreme Río Tinto. ISME J 5, 42-50.
464 Bi, X., Zhang, F., Shi, J., et al., 2016. Climatic change characteristics of Hechi city in
465   the last 56 years. Water Transf. Water Sci Technol 14, 105-110.
466 Bouzat, J.L., Hoostal, M.J., 2013. Evolutionary analysis and lateral gene transfer of

467 two-component regulatory systems associated with heavy-metal tolerance in
468 bacteria. J Mol Evol 76, 267-279.
469 Bordenave, S., Fourçans, A., Blanchard, S., et al., 2004. Structure and functional
470 analyses of bacterial communities changes in microbial mats following
471 petroleum exposure. Ophelia 58, 195-203.
472 Bordenave, S., Goñi-Urriza, M., Vilette, C., et al., 2008. Diversity of
473 ring-hydroxylating dioxygenases in pristine and oil contaminated microbial mats
474 at genomic and transcriptomic levels. Environ Microbiol 10, 3201-3211.
475 Bradshaw, A., 1997. Restoration of mined lands - using natural processes. Ecol Eng 8,
476 255-269.
477 Bruneel, O., Duran, R., Koffi, K., et al., 2005. Microbial diversity in a pyrite-rich
478 tailings impoundment (Carnoulès, France). Geomicrobiol J 22, 249-257.
479 Bruneel, O., Mghazli, N., Hakkou, R., et al., 2017. In-depth characterization of
480 bacterial and archaeal communities present in the abandoned Kettara pyrrhotite
481 mine tailings (Morocco). Extremophiles 21, 671-685.
482 Bruneel, O., Pascault, N., Egal, M., et al., 2008. Archaeal diversity in a Fe-As rich
483 acid mine drainage at Carnoulès (France). Extremophiles 12, 563-571.
484 Chao, Y., Liu, W., Chne, Y., et al., 2016. Structure, variation, and co-occurrence of
485 soil microbial communities in abandoned sites of a rare earth elements mine.
486 Environ Sci Technol 50, 11481-11490.
487 Chen, L., Li, J., Chen, Y., et al., 2013. Shifts in microbial community composition
488 and function in the acidification of a lead/zinc mine tailings. Environ Microbiol
489 15, 2431-2444.
490 China National Agricultural Technology Extension Center, 2006. Technical
491 specification for soil analysis (second edition). Beijing: China Agriculture Press
492 (in Chinese).
493 Ciarkowska, K., Gargiulo, L., Mele, G., 2016. Natural restoration of soils on mine
494 heaps with similar technogenic parent material: A case study of long-term soil
495 evolution in Silesian-Krakow Upland Poland. Geoderma 261, 141-150.
496 Clewell, A.F., 2000. Restoration of natural capital. Restor. Ecol. 8, 1-11.
497 Commission of the European Communities (COM), 2016. 593 Final. Proposal for a
498 directive of the European parliament and of the council on the management of
499 waste from the extractive industries. 2016/0280 (COD), Commission of the
500 European Communities, Brussels.
501 Dai, M., Martin, J.M., Cauwet, G., 2013. The significant role of colloids in the
502 transport and transformation of organic carbon and associated trace metals (Cd,
503 Cu and Ni) in the Rhône delta (France). Moussons: Recherche en Sciences
504 Humaines sur l'Asie du Sud-Est 51, 203-209.

505 Deng, C., Wang, S., Li, F., 2009. Research on soil multi-media environmental
506   pollution around a Pb-Zn mining and smelting plant in the karst area of Guangxi
507   Zhuang Autonomous Region, Southwest China. Acta Geochimica 28, 188-197.

508 Epelde, L., Lanzén, A., Blanco, F., et al., 2015. Adaptation of soil microbial
509   community structure and function to chronic metal contamination at an
510   abandoned Pb-Zn mine. FEMS Microbiol Ecol 91, 1-11.

511 Fan, M., Lin, Y., Huo, H., et al., 2016. Microbial communities in riparian soils of a
512   settling pond for mine drainage treatment. Water Res 96, 198-207.

513 Gan, H., Chew, T., Tay, Y., et al., 2012. Genome sequence of *Ralstonia* sp. strain pba,
514   a bacterium involved in the biodegradation of 4-aminobenzenesulfonate. J
515   Bacteriol 194, 5139-40.

516 Giloteaux, L., Goñi-Urriza, M., Duran, R., 2010. Nested PCR and new primers for
517   analysis of sulfate-reducing bacteria in low-cell-biomass environments. Appl
518   Environ Microbiol 76, 2856-2865.

519 Giloteaux, L., Duran, R., Casiot, C., et al., 2013. Three-year survey of
520   sulfate-reducing bacteria community structure in Carnoulès acid mine drainage
521   (France), highly contaminated by arsenic. FEMS Microbiol Ecol 83, 724-737.

522 Guan, N., Li, J., Shin, H.D., et al., 2017. Microbial response to environmental
523   stresses: From fundamental mechanisms to practical applications. Appl
524   Microbiol Biotechnol 101, 1-18.

525 Gupta, A., Dutta, A., Sarkar, J., et al., 2017. Metagenomic exploration of microbial
526   community in mine tailings of Malanjkhand copper project, India. Genomics
527   Data 12, 11-13.

528 Haferburg G., Kothe E, 2007. Microbes and metals: interactions in the environment. J
529   Basic Microbiol 47, 453-467.

530 Hansen, J., Grøn, C., Lund, U., et al. Uncertainty from sampling: workshop to launch
531   a Nordtest handbook on sampling uncertainty estimation and control. Accredit
532   Qual Assur 2007, 12(7):377-381.

533 Hao, X., Liang, Y., Yin, H., et al., 2017. Thin-layer heap bioleaching of copper
534   flotation tailings containing high levels of fine grains and microbial community
535   succession analysis. Int J Min Met Mater 24, 360-368.

536 Hou, D., Miao, B., Wang, Y., et al., 2012. Identification and analysis of zinc transport
537   genes in *Acidithiobacillus ferrooxidans*. Chin J Nonferrous Met 2012, 22,
538   1497-1502.

539 Huang L., Kuang J., Shu W., 2016. Microbial ecology and evolution in the acid mine
540   drainage model system. Trends Microbiol 24, 581-593.

541 Huang, L., Zhou, W., Hallberg, K., et al., 2011. Spatial and temporal analysis of the
542   microbial community in the tailings of a Pb-Zn mine generating acidic drainage.

543   Appl Environ Microbiol 77, 5540-4.

544 Hudson-Edwards, K., 2016. Tackling mine wastes. Science 352, 288-290.

545 Jiang, P., Lu, S., Tao, R., 2016. On analysis and strategies for tailing ponds in
546   Guangxi. Shanxi Architecture 42, 58-60.

547 Jin, Z., Li, Z., Li, Q., et al., 2015. Canonical correspondence analysis of soil heavy
548   metal pollution, microflora and enzyme activities in the Pb-Zn mine tailing dam
549   collapse area of Sidi village, SW China. Environ Earth Sci 73, 267-274.

550 Jorge, V., Pedroso, I., Quatrini, R., et al., 2008. *Acidithiobacillus*
551   *ferrooxidansmetabolism*: from genome sequence to industrial applications. BMC
552   Genomics 9, 597-597.

553 Kanehisa, M., Goto, S., Sato, Y., et al., 2014. Data, information, knowledge and
554   principle: back to metabolism in KEGG. Nucleic Acids Res 42, 199-205.

555 Keshri, J., Mankazana, B.B., Momba, M.N., 2015. Profile of bacterial communities in
556   South African mine-water samples using Illumina next-generation sequencing
557   platform. Appl Microbiol Biot 99, 3233-3242.

558 Kojima, H, Shinohara, A, Fukui, M., 2015. *Sulfurifustis* variabilis gen. nov. sp. nov. a
559   novel sulfur oxidizer isolated from a lake, and proposal of *Acidiferrobacteraceae*
560   fam. nov. and *Acidiferrobacterales* ord. nov. Int J Syst Evol Microbiol 65,
561   3709-3713.

562 Kojima, H, Watanabe, T, Fukui, M., 2016. *Sulfuricaulis limicola* gen. nov. sp. nov. a
563   sulfur oxidizer isolated from a lake. Int J Syst Evol Microbiol 66, 266-270.

564 Langille, M.G., Zaneveld, J., Caporaso, J., et al., 2013. Predictive functional profiling
565   of microbial communities using 16S rRNA marker gene sequences. Nat
566   Biotechnol 31, 814-21.

567 Lecumberri-Sanchez, P., Romer, R.L., Lüders, V., et al, 2014. Genetic relationship
568   between silver-lead-zinc mineralization in the Wutong deposit, Guangxi
569   province and Mesozoic granitic magmatism in the Nanling belt, southeast China.
570   Miner Deposita 49, 353-369.

571 Li, Q., Hu, Q., Zhang, C., 2015. The effect of toxicity of heavy metals contained in
572   tailing sands on the organic carbon metabolic activity of soil microorganisms
573   from different land use types in the karst region. Environ Earth Sci 74,
574   6747-6756.

575 Lima, A.T., Mitchell, K., O'Connell, D.W., et al., 2016. The legacy of surface
576   mining: remediation, restoration, reclamation and rehabilitation. Environ Sci
577   Policy 66, 227-233.

578 Liu, J., Yao, J., Wang, F., et al., 2018. China's most typical nonferrous organic-metal
579   facilities own specific microbial communities. Sci Rep 1, 12570-12580.

580 Liu, J., Zhang, X., Li, T., et al., 2014. Soil characteristics and heavy metal

581   accumulation by native plants in a Mn mining area of Guangxi, South China.
582   Environ Monit Assess 4, 2269-2279.

583 Liu, J., Zhang, M., Zhang, R., et al., 2016. Comparative studies of the composition of
584   bacterial microbiota associated with the ruminal content, ruminal epithelium and
585   in the faeces of lactating dairy cows. Microb Biotechnol 9, 257-268.

586 Mchardy, I.H., Goudarzi, M., Tong, M., et al., 2013. Integrative analysis of the
587   microbiome and metabolome of the human intestinal mucosal surface reveals
588   exquisite inter-relationships. Microbiome 1, 17-27.

589 Mergeay, M., Monchy, S., Vallaeys, T., 2010. *Ralstonia metallidurans*, a bacterium
590   specifically adapted to toxic metals: towards a catalogue of metal-responsive
591   genes. FEMS Microbiol Rev 27, 385-410.

592 Nakayama, J., 2010. Pyrosequence-based 16S rRNA profiling of gastrointestinal
593   microbiota. Biosci Microflora 29, 83-96.

594 Oudjehani, K., Zagury, G.J., Deschênes, L., 2002. Natural attenuation potential of
595   cyanide via microbial activity in mine tailings. Appl Microbiol Biot 58, 409-415.

596 Pan, X., Chen, Z., Li, L., et al., 2017. Microbial strategy for potential lead
597   remediation: A review study. World J. Microb. Biotechnol. 33, 35-42.

598 Rademaekers, K., Netherlands, E., Smakman, F., et al., 2011. Competitiveness of the
599   EU non-ferrous metals industries FWC sector competitiveness studies (final
600   report). European Commission, Directorate-General Enterprise and Industry.
601   http://ec.europa.eu/competition/consultations/2011_questionnaire_emissions_tra
602   ding/unicobre_annex1_en.pdf.

603 Ridl, J., Kolář, Michal, H., et al., 2016. Plants rather than mineral fertilization shape
604   microbial community structure and functional potential in legacy contaminated
605   soil. Front Microbiol 7. doi: 10.3389/fmicb.2016.00995.

606 Sandoval, P., Gabriel León, Isabel Gómez, et al., 2004. Transfer of RPS14 and RPL5
607   from the mitochondrion to the nucleus in grasses. Gene 324, 139-147.

608 Shu, W., Ye, Z., Lan, C., et al., 2001. Acidification of lead/zinc mine tailings and its
609   effect on heavy metal mobility. Environ Int 26, 389-394.

610 Sorokin, D.Y., Tourova, T.P., Mußmann, M., et al., 2008. *Dethiobacter alkaliphilus*
611   gen. nov. sp. nov., and *Desulfurivibrio alkaliphilus* gen. nov. sp. nov.: two novel
612   representatives of reductive sulfur cycle from soda lakes. Extremophiles 12,
613   431-439.

614 Sujkowska-Rybkowska, M., Ważny, R., 2018. Metal resistant rhizobia and
615   ultrastructure of *Anthyllis vulneraria* nodules from zinc and lead contaminated
616   tailing in Poland. Int J Phytoremediat 20, 709-720.

617 Theodoulou, F.L., Kerr, I.D., 2015. ABC transporter research: going strong 40 years
618   on. Biochem Soc T 43, 1033-1040.

619 Thorup, C., Schramm, A., Findlay, A.J., et al., 2017. Disguised as a sulfate reducer:
620   growth of the Deltaproteobacterium *Desulfurivibrio alkaliphilus* by sulfide
621   oxidation with nitrate. Mbio 8, e00671-17.

622 Trujillo, D.I., Silverstein, K.A.T., Young, N.D., 2014. Genomic characterization of
623   the LEED..PEEDs, a gene family unique to the *Medicago* lineage. G3-Genes
624   Genom. Genet 4, 2003-2012. http://doi.org/10.1534/g3.114.011874

625 Umezawa, K., Watanabe, T., Miura, A., et al., 2016. The complete genome sequences
626   of sulfur-oxidizing *Gammaproteobacteria Sulfurifustis variabilis*, skN76 T, and
627   *Sulfuricaulis limicola*, HA5 T. Stand Genomic Sci 11, 71-79.

628 Volant, A., Bruneel, O., Desoeuvre, A., et al., 2014. Diversity and spatiotemporal
629   dynamics of bacterial communities: physicochemical and other drivers along an
630   acid mine drainage. FEMS Microb Ecol 90, 247-263.

631 Vrutika, P., Anukriti, S., Rup, L., et al., 2016. Response and resilience of soil
632   microbial communities inhabiting in edible oil stress/contamination from
633   industrial estates. BMC Microbiol 16, 50-64.

634 Walder, I.F., Chavez, W.X., 1995. Mineralogical and geochemical behavior of mill
635   tailing material produced from lead-zinc skarn mineralization, Hanover, Grant
636   County, New Mexico, USA. Environ Geol 26, 1-18.

637 Wang, J., Yang, D., Yu, S., et al., 2007. Analysis on Karst rocky desertification in
638   upper reaches of Pearl River based on remote sensing. Sci Soil Water Conserv 5,
639   1-6.

640 Wang, T., 2018. Speciation changes of heavy metals in the process of tailings
641   ecological restoration in northwest Guangxi. MSc Thesis. University of Science
642   and Technology Beijing, Beijing, China.

643 Xiao, E., Krumins, V., Dong, Y., et al., 2016. Microbial diversity and community
644   structure in an antimony-rich tailings dump. Appl Microbiol Biotechnol 100,
645   7751-7763.

646 Yamanaka, T., 1996. Mechanisms of oxidation of inorganic electron donors in
647   autotrophic bacteria. Plant Cell Physiol 37, 569-574.

648 Yang, Z., Wu, Z., Liao, Y., et al., 2017. Combination of microbial oxidation and
649   biogenic schwertmannite immobilization: a potential remediation for highly
650   arsenic-contaminated soil. Chemosphere 181, 1-8.

651 Ye, S., Zeng, G., Wu, H., et al., 2017a. Biological technologies for the remediation of
652   co-contaminated soil. Crit Rev Biotechnol 37, 1062-1076.

653 Ye, S., Zeng, G., Wu, H., et al., 2017b. Co-occurrence and interactions of pollutants,
654   and their impacts on soil remediation-a review. Crit Rev Env Sci Tec 47,
655   1528-1553.

656 Ye, S., Zeng, G., Wu, H., et al., 2019. The effects of activated biochar addition on

657   remediation efficiency of co-composting with contaminated wetland soil. Resour

658   Conserv Recy 140, 278-285.

659 Yi, R., Cai, D., Zhang, Y., et al., 2016. Evaluation of biomonitoring methods using

660   benthic biatoms in Longjiang River, China. Chinese J Environ Eng 10,

661   3345-3353.

662 Yuan, L., Liu Y.S., 2016. The leaching principles of heavy metals in Pb-Zn tailings in

663   simulation acid rain. Environ Eng 30, 586-590.

664 Zacháry, D., Jordan, G., Völgyesi, P., et al., 2015. Urban geochemical mapping for

665   spatial risk assessment of multisource potentially toxic elements - a case study in

666   the city of Ajka, Hungary. J Geochem Explor 158, 186-200.

667 Zhan, J., Sun, Q.Y., 2014. Development of microbial properties and enzyme activities

668   in copper mine wasteland during natural restoration. Catena 116, 86-94.

669 Zhu, X., Yao, J., Wang, F., et al., 2018. Combined effects of antimony and sodium

670   diethyldithiocarbamate on soil microbial activity and speciation change of heavy

671   metals. Implications for contaminated lands hazardous material pollution in

672   nonferrous metal mining areas. J Hazard Materials 2018, 349, 160-167.

673   **Figure legends**

674   **Fig. 1.**   Sample location map (top left) and aerial photograph (top right) of the seven

675   tailings sites (T_3Y to T_31Y) close to Hechi city (● shown on map), Guangxi

676   (China), where the surface samples (◉ on aerial photo) were collected for the present

677   study. Field photographs of tailing sample sites are shown in the bottom panels (T_3Y

678   to T_31Y). As an example, T_3Y corresponds to the tailing sample code. T_3Y

679   means the tailing samples were taken from a three years old abandoned site

680   (not-used).

681

682   **Fig. 2.**   Relative abundances of bacterial phyla in the seven abandoned tailings sites.

683   The relative abundances of Alpha-, Beta-, Gamma-, Delta- *Proteobacteria*, and

684   *Actinobacteria* classes are shown in the insert diagram.

685

686   **Fig. 3.**   (A) Non-metric multidimensional scaling (NMDS) analysis of bacterial

687   communities in seven tailings sites at genus level. (B) Distance-based redundancy

688   analysis (db-RDA) of genus and selected geochemical factors in seven tailings sites.

689   Both NMDS and db-RDA analysis were based on the weighted normalized unifrac

690   distance algorithms. Direction and magnitude of arrows indicate the correlation of

691   geochemical factors and genera.

692

693   **Fig. 4.**   (A) Network analysis for the detected bacterial communities (genus level) in

694   different tailings sites. Color was coded by tailings sites. Each node indicates one

695   genus. Colors of node represent the different major phyla. The size the species-node

696   denotes abundance of species. Black nodes represented the no_rank/un-classified

697   genera which were shared by tailings sites. Light green nodes represented the

698   no_rank/un-classified genera, which were specific in different tailings sites. The

699   degree of node was assessed by the numbers of nodes connected directly to that node.

700   The more lines on the node denotes the higher degree of correlation between the sites

701   and other genera. (B) The sub-network analysis for modularity of genera. Colors of

702   node represent the different module. Node size is proportional to the modularity class.

703   The nodes without labels represented the no_rank/un-classified genera. B. P.,

704   *Burkholderia-Paraburkholderia*

705

706   **Fig. 5.**   Correlation analysis based on the Pearson test showing the relation between

707   the geochemical factors and the relative abundance of bacterial communities at the

708   phylum (A) and genus (B) levels. Only the top 30 bacterial communities are shown in

709   this figure. Color key for the correlation values is shown on the right panel inset;

710   positive correlations are in red text, negative correlations are in green, non-significant

711   correlations are shown in white. * $0.01 < p \leq 0.05$, ** $0.001 < p \leq 0.01$, *** $p \leq 0.001$

712

713   **Fig. 6**   Principal Components Analysis (PCA) for bacterial community structure and

714   KEGG metabolic functional pathways based on 16S rRNA sequencing reads.
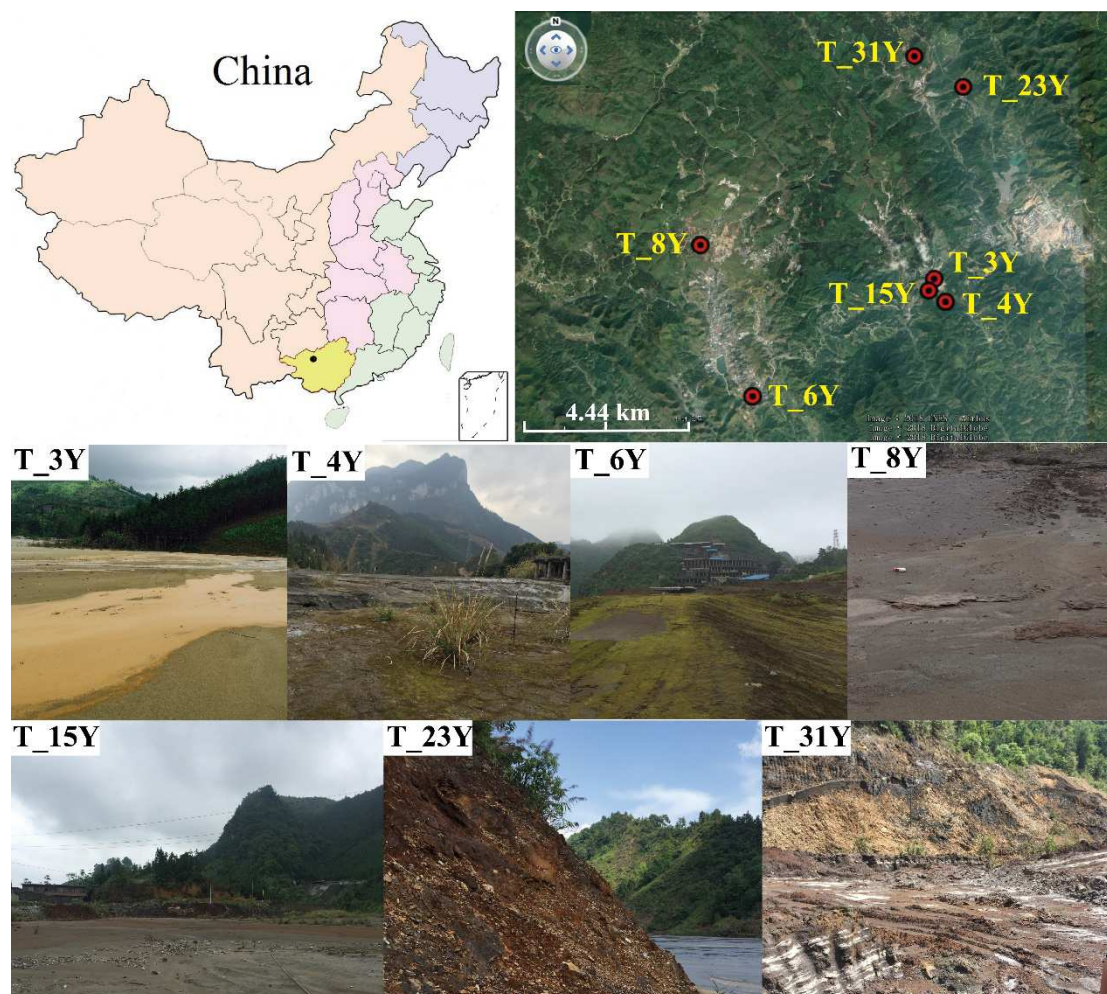
Fig. 1. Sample location map (top left) and aerial photograph (top right) of the seven tailings sites (T_3Y to T_31Y) close to Hechi city (● shown on map), Guangxi (China), where the surface samples (⦿ on aerial photo) were collected for the present study. Field photographs of tailing sample sites are shown in the bottom panels (T_3Y to T_31Y). As an example, T_3Y corresponds to the tailing sample code. T_3Y means the tailing samples were taken from a three years old abandoned site (not-used).

723
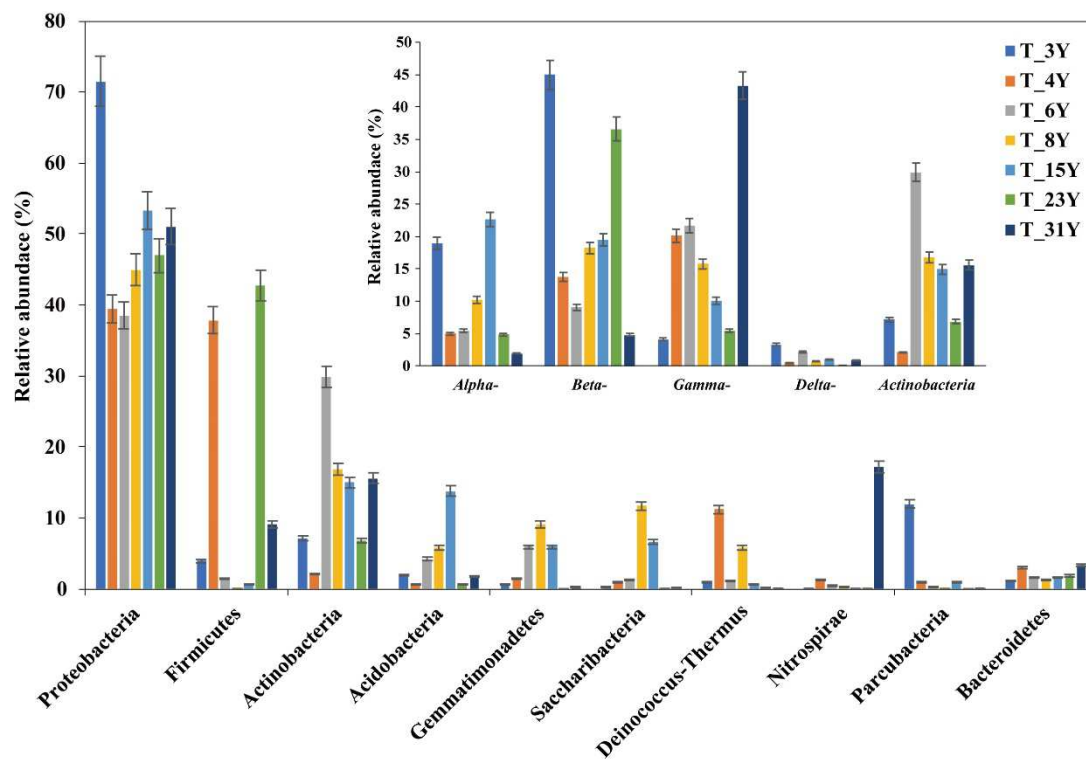
Fig. 2. Relative abundance of bacterial communities at phylum level in the seven abandoned tailings sites. Relative abundance of Alpha-, Beta-, Gamma-, Delta-*Proteobacteria*-related and *Actinobacteria* classes are shown in the map inset.
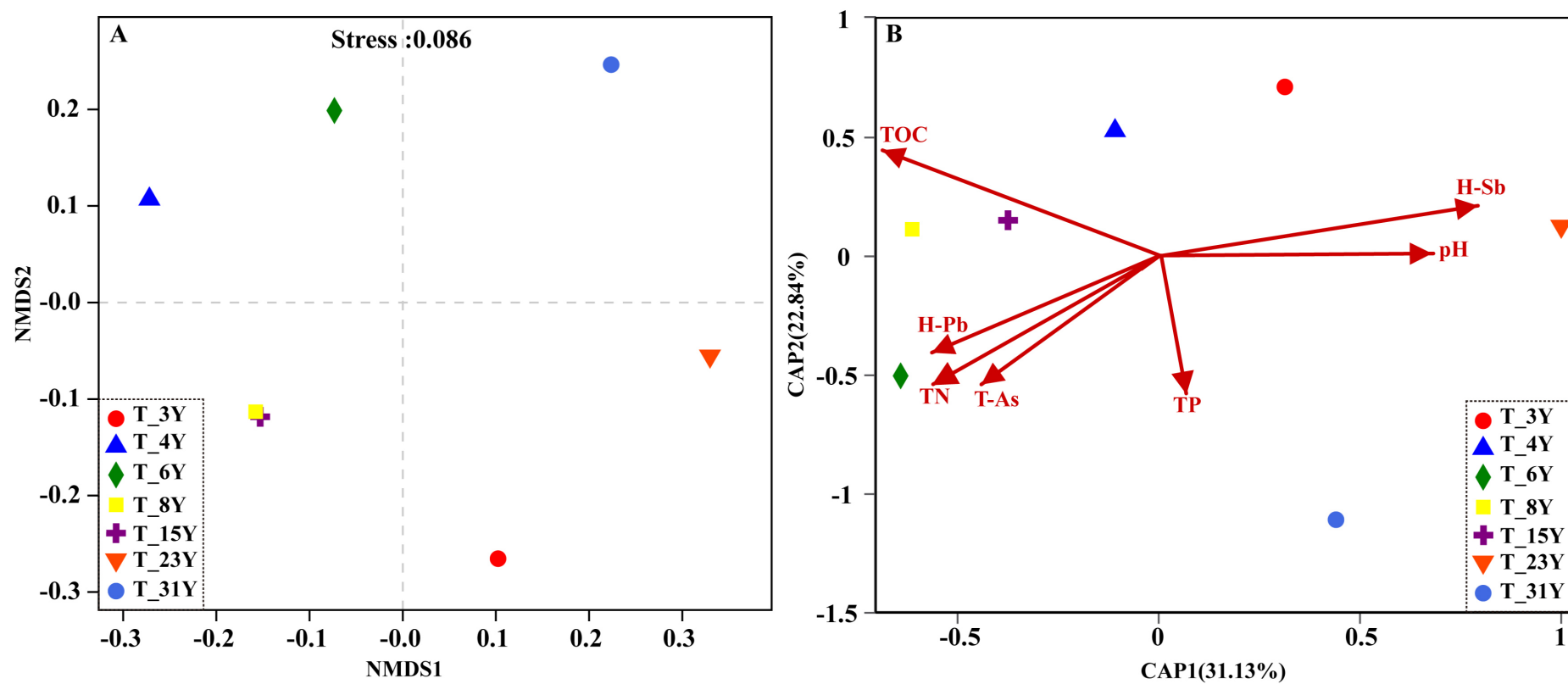
**Fig. 3.** (A) Non-metric multidimensional scaling (NMDS) analysis of bacterial communities in seven tailings sites at genus level. (B) Distance-based redundancy analysis (db-RDA) of genus and selected geochemical factors in seven tailings sites. Both NMDS and db-RDA analysis were based on the weighted normalized unifrac distance algorithms. Direction and magnitude of arrows indicate the correlation of geochemical factors and genera.
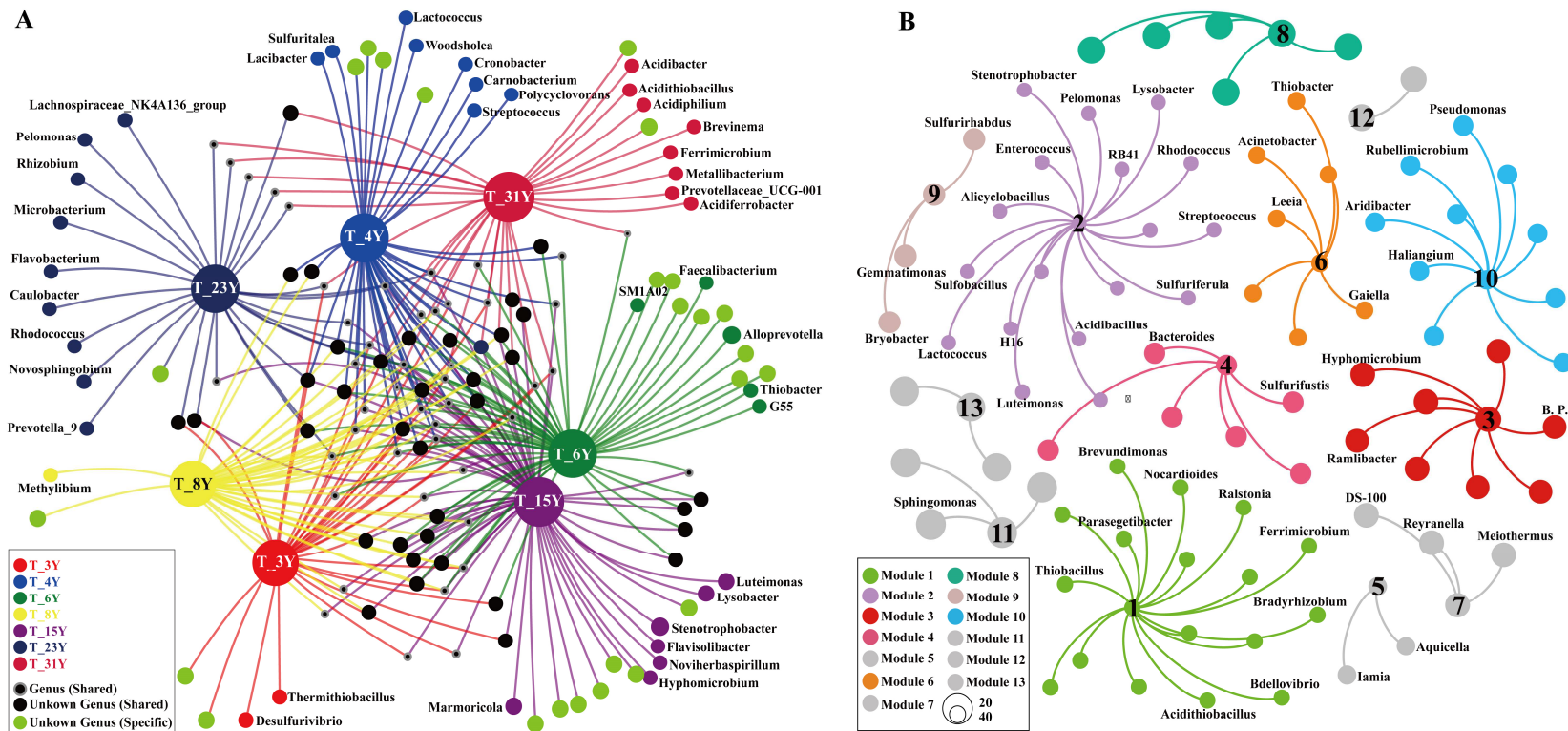
Fig. 4. (A) Network analysis for the detected bacterial communities (genus level) in different tailings sites. Color was coded by tailings sites. Each node indicates one genus. Colors of node represent the different major phyla. The size the species-node denotes abundance of species. Black nodes represented the no_rank/un-classified genera which were shared by tailings sites. Light green nodes represented the no_rank/un-classified genera, which were specific in different tailings sites. The degree of node was assessed by the numbers of nodes connected directly to that node. The more lines on the node denotes the higher degree of correlation between the sites and other genera. (B) The sub-network analysis for modularity of genera. Colors of node represent the different module. Node size is proportional to the modularity class. The nodes without labels represented the no_rank/un-classified genera. B. P., *Burkholderia-Paraburkholderia*
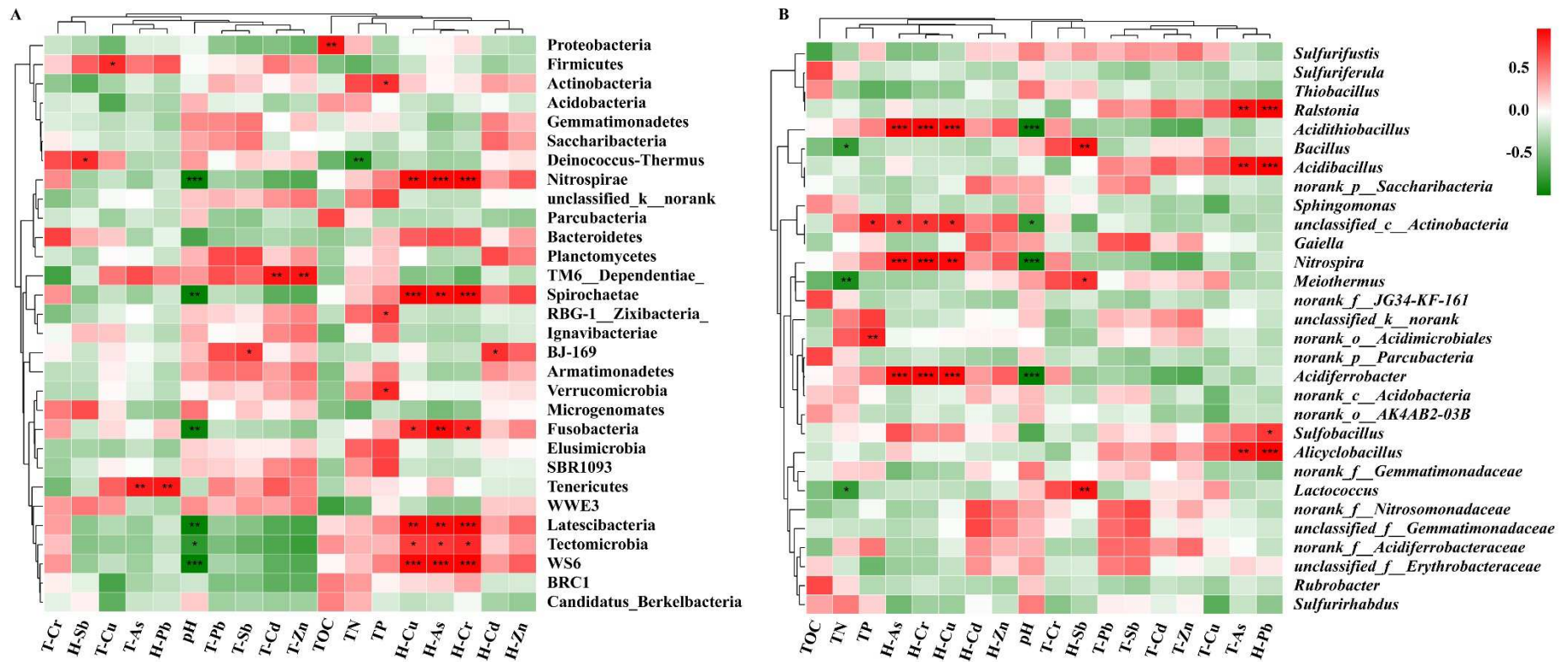
740
741 **Fig. 5**. Correlation analysis based on the Pearson test showing the relation between the geochemical factors and the relative abundance of
742 bacterial communities at the phylum (A) and genus (B) levels. Only the top 30 bacterial communities are shown in this figure. Color key for the
743 correlation values is shown on the right panel inset; positive correlations are in red text, negative correlations are in green, non-significant
744 correlations are shown in white. * $0.01 < p \leq 0.05$, ** $0.001 < p \leq 0.01$, *** $p \leq 0.001$
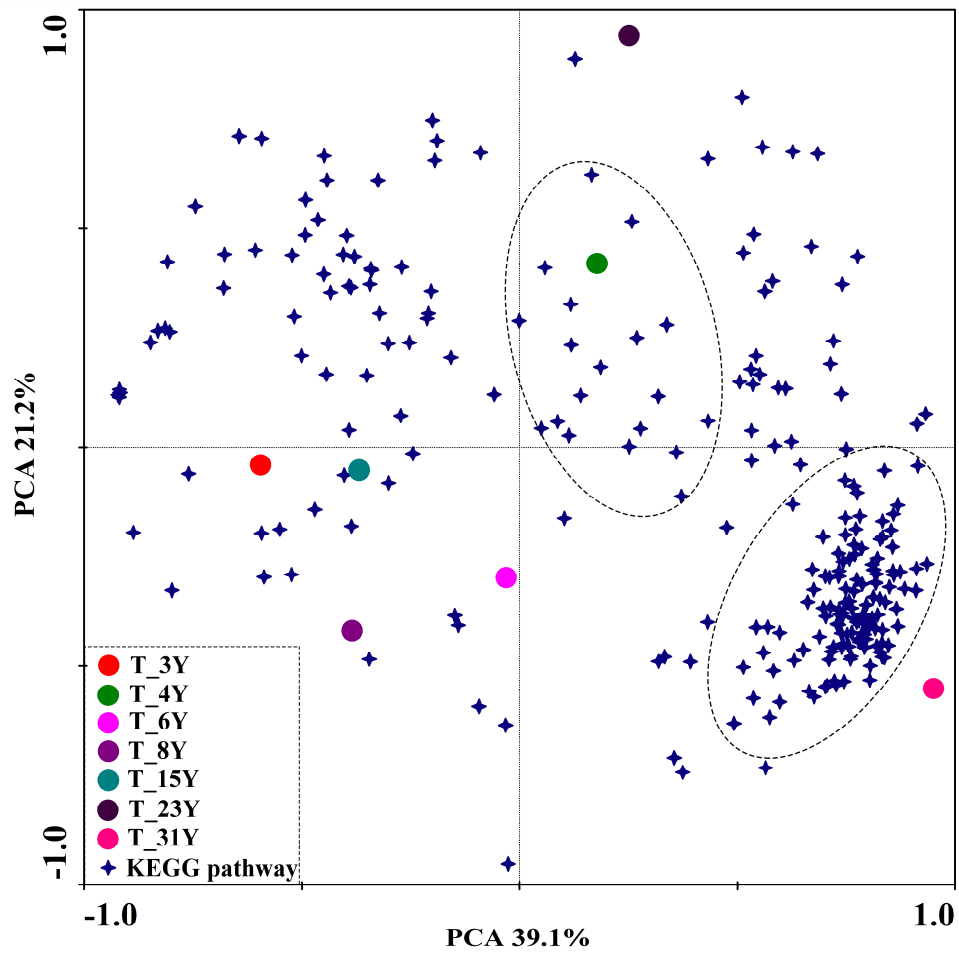
Fig. 6 Principal Components Analysis (PCA) for bacterial community structure and KEGG metabolic functional pathways based on 16S rRNA sequencing reads.

748 **Table 1**

749 Spearman correlation analysis for geochemical factor variables and a-diversity index

750 ($p < 0.05$).

Variables used in analysis	Correlated variables |*rho*|>0.75	*rho*	*p*-value
TOC	H-Cr	0.786[*]	0.036
T-As	T-Cd	0.786[*]	0.036
	T-Cr	-0.821[*]	0.023
	T-Zn	0.857[*]	0.014
T-Cd	T-Cu	0.786[*]	0.036
	T-Zn	0.929[**]	0.003
	H-Cr	-0.893[**]	0.007
T-Pb	H-Cd	0.821[*]	0.023
	H-Pb	0.821[*]	0.023
T-Zn	H-Cr	-0.893[**]	0.007
H-Cd	H-Cu	0.929[**]	0.003
	H-Zn	0.929[**]	0.003
H-Cu	H-Zn	0.929[**]	0.003
ace	PD	0.964**	0.0004
PD	TP	-0.786*	0.036

751 TOC, total organic carbon; TN, total nitrogen; TP, total phosphorus; T-(metal), total content of

752 metal(loid)s; H-(metal), the acid extraction of metal(loid)s; ace, microbial richness; PD,

753 phylogenetic diversity; *rho*, Spearman coefficient of product-moment correlation

754 **Table 2**

755 Main genus contributed to the differences between different bacterial communities of

756 tailings sites with different abandoned time. The relative abundances of genera ≥ 1 at

757 least at one tailing site are shown.

Genus	Contrib (%)								
	a & b	a & c	a & d	a & e	b & c	b & d	b & e	c & d	c & e
Dissi	68.3	68.4	59.2	73.5	52.7	56.9	83.2	49.6	78.5
Acidibacillus	-	-	-	3.65	-	-	3.15	-	2.98
Acidiferrobacter	-	-	-	2.52	-	-	2.17	-	2.06
Acidithiobacillus	-	-	-	3.78	-	-	3.27	-	3.09
Acinetobacter	0.93	0.69	0.75	0.97	-	0.70	1.56	0.73	1.37
Alicyclobacillus	-	-	-	2.81	-	-	2.43	-	2.30
Bacillus	7.34	-	0.67	0.40	8.17	7.89	5.36	0.71	-
Bdellovibrio	2.37	1.81	2.18	2.47	-	-	-	-	-
Burkholderia-Par	-	-	-	1.63	-	-	1.59	-	1.28
DS-100	-	1.59	1.34	-	2.04	1.38	-	1.04	1.37
Enterococcus	1.51	0.96	-	-	-	1.87	1.14	1.43	0.76
Erysipelothrix	3.04	2.70	3.33	1.96	-	-	0.68	-	-
Gaiella	-	4.48	5.01	-	4.59	4.01	0.78	1.79	3.73
Gemmatimonas	0.58	-	1.12	0.90	1.22	1.79	-	0.60	1.11
Iamia	0.82	2.75	0.67	-	2.56	-	0.47	2.88	2.12
Lactococcus	4.89	-	-	-	2.68	5.45	3.75	-	-
Meiothermus	3.54	0.59	2.09	1.57	3.23	2.39	4.11	2.13	1.78
Nitrospira	1.18	0.98	-	2.77	-	0.75	2.40	0.68	2.27
Ralstonia	0.81	-	-	-	-	-	3.68	-	3.11
Rhodococcus	-	-	-	1.35	-	-	1.29	-	1.22
Rubellimicrobium	-	-	1.09	0.44	-	-	-	-	-
Rubrobacter	3.91	2.66	3.16	3.54	1.02	1.13	-	-	0.68
Sphingomonas	-	0.65	3.91	1.42	1.18	-	0.98	-	1.70
Sulfobacillus	-	-	-	3.27	-	-	2.82	-	2.67
Sulfuriferula	8.46	8.20	10.3	7.57	-	0.96	0.91	-	0.86
Sulfurifustis	5.39	7.09	5.18	0.44	2.93	1.92	4.57	3.74	6.25
Sulfurirhabdus	1.69	1.12	1.11	1.53	-	3.01	-	-	-
Thermithiobacillus	2.84	2.52	3.11	2.56	-	-	-	-	-
Thiobacillus	1.97	3.53	0.65	5.07	2.27	1.53	2.84	3.87	1.20
Thiobacter	-	2.40	-	-	2.46	-	0.41	2.59	2.00

758 Contrib, the contribution of each genus to the differences of bacterial communities of tailings sites;

759 a, T_3Y; b, T_4Y; c, T_6Y; d, T_8Y and T_15Y; e, T_23Y and T_31Y; "-", the contribution data

760 < 0.4.

761 **Table 3**

762 Correlation analysis of modules eigengenes in the bacterial community network (Fig.

763 4) and selected geochemical factors by BIOENV analysis and Monte-Carlo test.

Combination of geochemical factors		Module 1	Module 2	Module 3
T-As	rM	0.51	0.29	0.54
	p	0.07	0.28	0.10
TOC + H-Pb	rM	0.32	0.58	0.59
	p	0.20	0.03	0.07
pH + TOC + H-Pb	rM	0.84	0.33	0.26
	p	0.01	0.11	0.19
TOC + H-Pb + T-As	rM	0.37	0.53	0.62
	p	0.16	0.06	0.08
pH + TOC + H-Pb + T-As	rM	0.80	0.37	0.48
	p	0.01	0.10	0.13
TOC + H-Pb + T-As + H-Sb	rM	0.27	0.69	0.51
	p	0.23	0.08	0.13

764

Highlights:

- Specific bacterial communities were observed according to tailing age

- S/Fe-oxidizing and metal(loid)-related bacteria abundance increased with tailings age

- Genera beneficial to plant growth were detected

- Bacterial communities harbored adaptive DNA repair and recombination functions